

Very Long Baseline Neutrino Oscillation Experiment for Precise Measurements of Mixing Parameters and CP Violating Effects

M.V. Diwan, D. Beavis, Mu-Chun Chen, J. Gallardo, R.L. Hahn, S. Kahn, H. Kirk, W. Marciano,
W. Morse, Z. Parsa, N. Samios, Y. Semertzidis, B. Viren, W. Weng, P. Yamin, M. Yeh
Physics Department, Brookhaven National Laboratory, Upton, NY 11973

W. Frati, K. Lande, A.K. Mann, R. Van Berg, P. Wildenhain
Department of Physics and Astronomy, University of Pennsylvania, Philadelphia, PA 19104

J.R. Klein
Department of Physics, University of Texas, Austin Texas 78712

I. Mocioiu
Physics Department, University of Arizona, Tucson, AZ 85721

R. Shrock
C. N. Yang Institute for Theoretical Physics, State University of New York, Stony Brook, NY 11794

K.T. McDonald
Joseph Henry Laboratories, Princeton University, Princeton, NJ 08544

We analyze the prospects of a feasible, Brookhaven National Laboratory based, very long baseline (BVLB) neutrino oscillation experiment consisting of a conventional horn produced low energy wide band beam and a detector of 500 kT fiducial mass with modest requirements on event recognition and resolution. Such an experiment is intended primarily to determine CP violating effects in the neutrino sector for 3-generation mixing. We analyze the sensitivity of such an experiment. We conclude that this experiment will allow determination of the CP phase δ_{CP} and the currently unknown mixing parameter θ_{13} , if $\sin^2 2\theta_{13} \geq 0.01$, a value ~ 15 times lower than the present experimental upper limit. In addition to θ_{13} and δ_{CP} , the experiment has great potential for precise measurements of most other parameters in the neutrino mixing matrix including Δm_{32}^2 , $\sin^2 2\theta_{23}$, $\Delta m_{21}^2 \times \sin 2\theta_{12}$, and the mass ordering of neutrinos through the observation of the matter effect in the $\nu_\mu \rightarrow \nu_e$ appearance channel.

PACS numbers: 12.15.Ff, 13.15.+g, 14.60.Lm, 14.60.Pq, 11.30.Fs, 11.30.Er

Introduction

Measurements of solar and atmospheric neutrinos have provided strong evidence for non-zero neutrino masses and mixing [1–3]. Atmospheric results have been further strengthened by the K2K collaboration’s accelerator based results [4]. The Solar neutrino results have been confirmed by the KamLAND collaboration in a reactor based experiment that has shown that the large mixing angle (LMA) solution is most likely the correct one [5]. Interpretation of the experimental results is based on oscillations of one neutrino flavor state, ν_e, ν_μ or ν_τ , into the others, and described quantum mechanically in terms of neutrino mass eigenstates, ν_1, ν_2 and ν_3 . The mass squared differences involved in the transitions are measured to be approximately $\Delta m_{21}^2 \equiv m(\nu_2)^2 -$

$m(\nu_1)^2 = (5 - 20) \times 10^{-5} \text{eV}^2$ for the solar neutrinos and $\Delta m_{32}^2 \equiv m(\nu_3)^2 - m(\nu_2)^2 = \pm(1.6 - 4.0) \times 10^{-3} \text{eV}^2$ for the atmospheric neutrinos, with large mixing strengths, $\sin^2 2\theta_{12} \approx 0.86$ and $\sin^2 2\theta_{23} \approx 1.0$ in both cases.

These existing data on neutrino oscillations[1–3] and the prospect of searching for CP violation make clear that the next generation of oscillation experiments must be significantly more ambitious than before. In particular, the source of neutrinos needs to be accelerator based so that both the neutrino flavor content and the energy spectrum of the initial state can be selected. Several approaches have been explored in the literature. These involve either a narrow band “off-axis” beam produced with a conventional magnetic focusing system [6–8] or a neutrino factory based on a muon storage ring [9]. In this paper, we show that the currently favored param-

eters open the possibility for an accelerator based very long baseline (BVLB) experiment that can explore both solar and atmospheric oscillation parameters in a single experiment, complete the measurement of the mixing parameters, and search for new physics.

The Experimental Strategy

There are four measurements of primary interest that can be addressed with the experimental arrangement described in this paper. Using the parameter convention described in [1], they are:

- (i) Definitive observation of oscillatory behavior (multiple oscillations) in the ν_μ disappearance mode and precise determination of the oscillation parameters Δm_{32}^2 and $\sin^2 2\theta_{23}$, with statistical errors $\sim \pm 1\%$.
- (ii) Detection of the oscillation $\nu_\mu \rightarrow \nu_e$ in the appearance mode and measurement of the parameter $\sin^2 2\theta_{13}$. This will involve matter enhancement and also allow definitive measurement of the sign of Δm_{32}^2 , i.e., which neutrino ν_3 or ν_2 is heavier.
- (iii) Measurement of the CP violation parameter, δ_{CP} , in the lepton sector.
- (iv) Measurement of $\Delta m_{21}^2 \times \sin 2\theta_{12}$ in the appearance channel of $\nu_\mu \rightarrow \nu_e$.

We describe how these measurements could be carried out with good precision in a single accelerator based experiment. For precise and definitive measurement of oscillations we must observe multiple oscillation nodes in the energy spectrum of reconstructed muon and electron neutrino charged current events. The multiple node signature is also necessary in order to distinguish between oscillations and other more exotic explanations such as neutrino decay [10] or extra dimensions [11] for the muon neutrino deficit in atmospheric neutrinos. Since the cross-section, Fermi motion, and nuclear effects limit the statistics and the energy resolution (for reconstructed neutrino energy) of low energy charged current events, we use neutrinos with energies greater than few hundred MeV and clean events with a single visible muon or electron that are dominated by quasielastic scattering, $\nu_l + n \rightarrow l + p$, where l denotes a lepton. Figure 1 shows that the distance needed to observe at least 3 nodes in the reconstructed neutrino energy spectrum is greater than

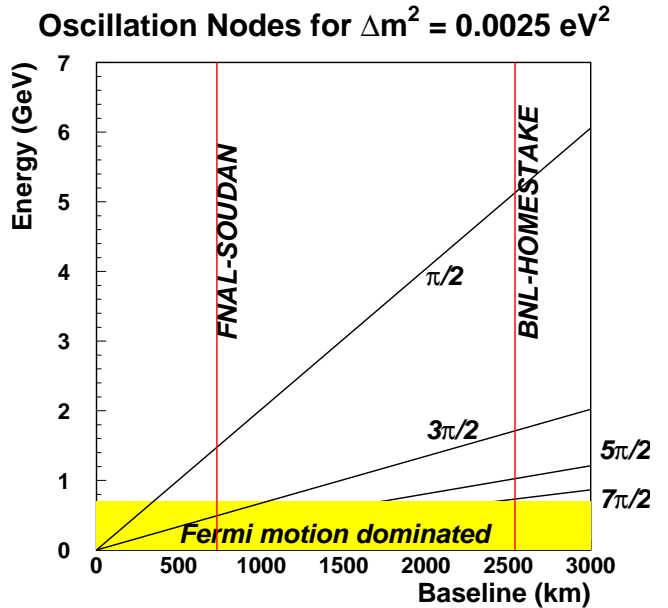


FIG. 1: (color) Nodes of neutrino oscillations for disappearance (not affected by matter effects) as a function of oscillation length and energy for $\Delta m_{32}^2 = 0.0025 \text{ eV}^2$. The distances from FNAL to Soudan and from BNL to Homestake are shown by the vertical lines.

2000 km for $\Delta m_{32}^2 = 0.0025 \text{ eV}^2$, the currently favored value from Super-Kamiokande atmospheric data [2]. A baseline of longer than 2000 km coupled with a wide band beam with high flux from 0.5 to 6 GeV will provide a nodal pattern in the $\nu_\mu \rightarrow \nu_\mu$ disappearance channel and good sensitivity over a broad range of Δm_{32}^2 .

The low energy wide band beam and the very long baseline also have a number of important advantages for the appearance channel of $\nu_\mu \rightarrow \nu_e$. These advantages can be summarized using Figure 2 which shows the probability of $\nu_\mu \rightarrow \nu_e$ oscillation as a function of neutrino energy for the distance of 2540 km, the distance between BNL and the Homestake mine in South Dakota. The oscillation parameters that we have assumed are indicated in the figure and the caption. We define the natural mass ordering (*NO*) of neutrinos to be $m_3 > m_2 > m_1$, and the other two possibilities ($m_2 > m_1 > m_3$ and $m_1 > m_2 > m_3$) are collectively called reversed ordering (*RO*). Both *RO* possibilities have very similar physical consequences, but $m_1 > m_2 > m_3$ is strongly disfavored by the explanation of the Solar neutrino deficit using matter enhanced neutrino oscillation (the LMA solution). Since neutrinos from an accelerator beam must

Proposed Experimental Configuration

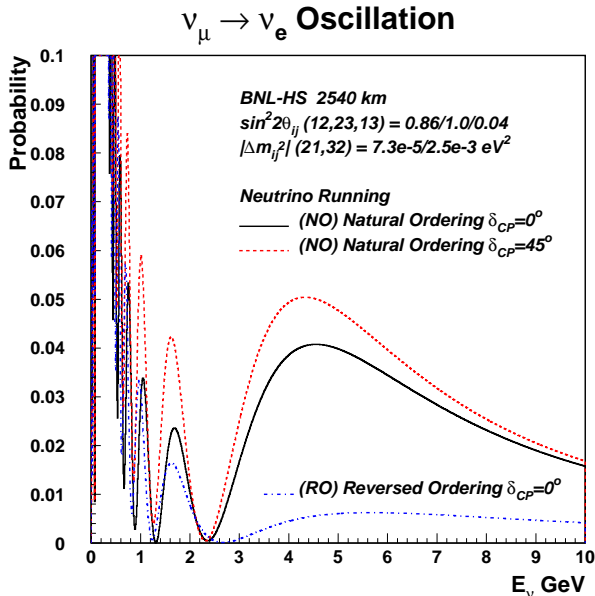


FIG. 2: (color) Probability of $\nu_\mu \rightarrow \nu_e$ oscillations at 2540 km. The calculation includes the effects of matter. The dotted ($\delta_{CP} = 45^\circ$) and solid ($\delta_{CP} = 0^\circ$) curves are for *NO* and the lower dot-dashed ($\delta_{CP} = 0^\circ$) curve is for *RO*. The parameters used for the figure are $\sin^2 2\theta_{12} = 0.86$, $\sin^2 2\theta_{23} = 1.0$, and $\sin^2 2\theta_{13} = 0.04$ and $\Delta m_{21}^2 = 7.3 \times 10^{-5} eV^2$, $\Delta m_{32}^2 = 0.0025 eV^2$.

pass through the Earth to arrive at a detector located 2540 km away, the probability in Figure 2 includes the effects of matter, which enhance (suppress) the probability above 3.0 GeV for *NO* (*RO*) [12]. Therefore the appearance probability above 3.0 GeV is sensitive to both the mass ordering and the parameter $\sin^2 2\theta_{13}$. The probability in the region 1.0 to 3.0 GeV is less sensitive to matter but much more sensitive to the CP phase δ_{CP} as shown in Figure 2[13]. The increase in the probability below 1.5 GeV is due to the presence of terms involving the solar oscillation parameters, Δm_{21}^2 and $\sin^2 \theta_{12}$. Therefore, the spectrum of electron neutrino events measured with a wide band beam over 2540 km with sufficiently low background has the potential to determine $\sin^2 2\theta_{13}$, δ_{CP} , and the mass ordering of neutrinos as well as Δm_{21}^2 because these parameters affect different regions of the energy spectrum. In the following, we examine how well the parameters can be determined and the implications for the detector performance and background.

The high energy proton accelerator, to be used for making the neutrino beam, must be intense (~ 1 MW in power) to provide sufficient neutrino-induced event rates in a massive detector very distant from it. Such a long baseline experimental arrangement [14] may be realized with a neutrino beam from the upgraded 28 GeV proton beam from the Alternating Gradient Synchrotron at the Brookhaven National Laboratory (BNL) and a water Cherenkov detector with 0.5 megaton of fiducial mass at either the Homestake mine in South Dakota or the Waste Isolation Pilot Plant (WIPP) in New Mexico, at distances ~ 2540 km and ~ 2900 km from BNL, respectively. A version of the detector is described at length in [15] and is a candidate for location in the Homestake Mine, where it would occupy five independent cavities, each about 100 kton in fiducial volume. Another version of the detector in a single volume is described in [16]. For much of the discussion below we have used the distance of 2540 km to Homestake for our calculations. Although the statistics obtained at 2900 km to WIPP will be somewhat smaller, many of the physics effects will be larger, and therefore the resolution and the physics reach of the BVLB experiment are approximately independent of the choice between Homestake or WIPP.

The accelerator upgrade as well as the issues regarding the production target and horn system are described in [17]. We briefly describe it here for completeness. Currently, the BNL-AGS can accelerate $\sim 7 \times 10^{13}$ protons upto 28 GeV approximately every 2 sec. This corresponds to average beam power of about 0.16 MW. This average power could be upgraded by increasing the repetition rate of the AGS synchrotron to 2.5 Hz while keeping the number of protons per pulse approximately the same. Currently a 200 MeV room temperature LINAC in combination with a small synchrotron, called the Booster, injects protons into the AGS at 1.2 GeV. The process of collecting sufficient number of protons from the Booster into the AGS takes about 0.6 sec. Therefore, for 2.5 Hz operation the Booster must be replaced by a new injector. A new super-conducting LINAC to replace the Booster could serve the role of a new injector; the remaining modifications to the AGS are well understood and they involve power supplies, the RF system, and other rate dependent systems to make the accelerator ramp up and down at 2.5 Hz. We expect the final upgraded accelerator configuration to yield

8.9×10^{13} protons every 400 ms at 28 GeV. Our studies show that this intensity can be further upgraded to 2 MW by incremental improvements to the LINAC and the AGS repetition rate.

In addition to the 1 MW accelerator upgrade, the pion production target, the horn focusing system, and the decay tunnel, which must be aimed at an angle of 11.26 degrees into the earth (towards Homestake) need to be built. Our current studies indicate that a carbon-carbon composite target inserted into a conventional aluminum horn cooled with forced Helium and water will function in the 1 MW beam for a sufficient length of time. Our current plan is to build a hill instead of an underground tunnel to accommodate the 200 m long pion decay tunnel. We consider both the rapid cycling accelerator upgrade which maintains a relatively low intensity per pulse and the 1 MW capable target technically less risky than other alternatives. For comparison, at JPARC [18] the first (preliminary) stage of 0.75 MW is to be achieved at $\sim 1/3$ Hz with 3.3×10^{14} protons per pulse at 50 GeV. At Fermilab a 2 MW upgrade to the 120 GeV main injector calls for either an 8 GeV super-conducting LINAC or a new rapid cycling proton synchrotron as injectors for the main injector[19]. As explained in the following, the combination of the very long baseline and a 500 kT detector allows the BVLB experiment to use a lower average power at 1 MW compared to the proposed JPARC or NuMI(Off axis) [7] projects and achieve wider physics goals. This reduces the technical difficulties (liquid mercury or moving targets, radiation damage, shielding of personnel, etc.) associated with using beam powers in excess of 1 MW.

We have performed detailed simulations of a wide band horn focused neutrino beam using 1 MW of 28 GeV protons on a graphite target. The neutrino spectrum obtained in these simulations and used for the results in this paper is shown in Figure 3 normalized for POT (protons on target). We calculate that with such a beam (total intensity of $\sim 4.7 \times 10^{-5} \nu/m^2/POT$ at distance of 1 km from the target) we will obtain about 60,000 charged current and 20,000 neutral current events in a total exposure lasting 5×10^7 seconds in a 0.5 megaton water Cherenkov detector located at the Homestake mine 2540 km away from BNL. For the results reported below, we use the particle spectra obtained by making cuts to select single muon or electron quasielastic events. Events with multiple particles (about 4 times higher in statistics) could be used to further enhance the statistical significance of the

BNL Wide Band. Proton Energy = 28 GeV

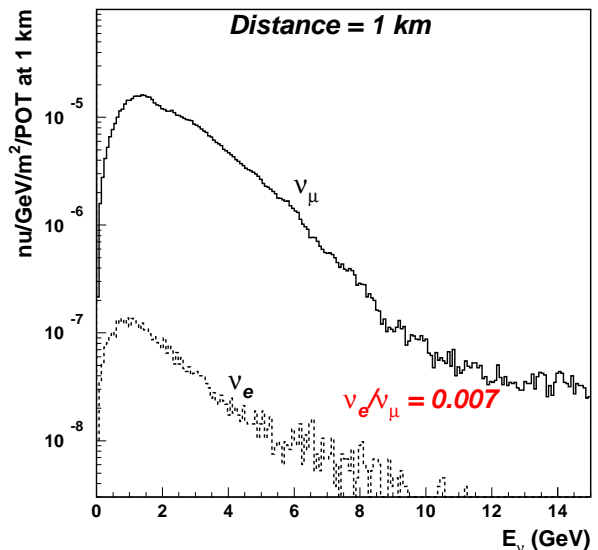


FIG. 3: (color) The simulated wide band neutrino flux for 28 GeV protons on a graphite target used for the calculations in this paper. (POT=protons on target).

effects.

A conventional horn focused beam can be run in either the neutrino or the anti-neutrino mode. In this paper we show that most of the physics program in the case of 3-generation mixing can be carried out by taking data in the neutrino mode alone. It is well known that experiments that must take data with anti-neutrinos, which have lower cross section, must run for long times to accumulate sufficient statistics [7]. This problem is largely alleviated in our method. We will discuss the anti-neutrino beam in a separate paper; here we wish to focus on the physics reach of the neutrino beam alone [20].

ν_μ Disappearance

An advantage of the very long baseline is that the multiple node pattern is detectable over the entire allowed range of Δm_{32}^2 . The sensitivity to $\Delta m_{32}^2 \sim 1.24 \frac{E_\nu [\text{GeV}]}{L [\text{km}]} \text{ eV}^2$ extends to the low value of about $5 \times 10^{-4} \text{ eV}^2$, significantly below the allowed range from Super Kamiokande. At energies lower than ~ 1 GeV, the ν_μ energy resolution will be dominated by Fermi motion and nuclear effects, as illustrated in Figure 1. The contribution to the resolution from water Cherenkov track recon-

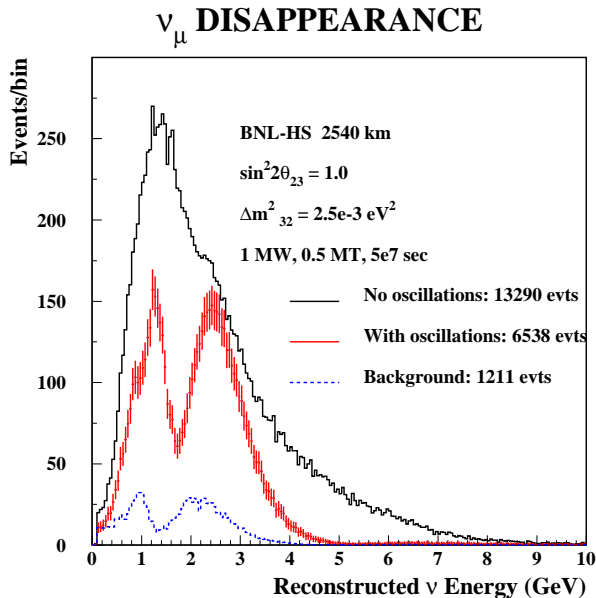


FIG. 4: (color) Spectrum of expected single muon events in a 0.5 MT water Cherenkov detector at 2540 km from the source. We have assumed 1 MW of beam power and 5×10^7 sec of data-taking. The top histogram is without oscillations; the middle histogram with error bars is with oscillations. Both histograms include the dominant single pion charged current background. The bottom histogram shows this background contribution to the oscillating spectrum. This plot is for $\Delta m^2_{32} = 0.0025 \text{ eV}^2$. The error bars correspond to the statistical error expected in the bin. At low energies the Fermi movement, which is included in the simulation, will dominate the resolution.

struction depends in first approximation on the photomultiplier tube coverage. With coverage greater than 10%, a reconstruction energy resolution of better than $\sim 10\%$ should be achieved [6]. The simulated spectrum of the expected ν_μ disappearance signal including backgrounds and resolution is shown in Figure 4 for $\Delta m^2_{32} = 0.0025 \text{ eV}^2$ as a function of reconstructed neutrino energy. The background, which will be primarily charged current events, will also oscillate and broaden the dips in the nodal pattern. From this spectrum we estimate that the determination of Δm^2_{32} will have a statistical uncertainty of approximately $\pm 0.7\%$ at

$\Delta m^2_{32} = 0.0025 \text{ eV}^2$ and $\sin^2 2\theta_{23} = 1$. The experiment can determine $\sin^2 2\theta_{23} > 0.99$ at 90% confidence level. Within the parameter region of interest there will be little correlation in the determination of Δm^2_{32} and $\sin^2 2\theta_{23}$. The precision of the experiment is compared in Figure 5 with the precision expected from MINOS [21] and the result from Super-Kamiokande [2]. Since the statistics and the size of the expected signal (distortion of the spectrum) are both large in the disappearance measurement, we expect that the final error on the parameters will be dominated by the systematic error. A great advantage of the very long baseline and multiple oscillation pattern in the spectrum is that the effect of systematic errors on flux normalization, background subtraction, and spectrum distortion due to nuclear effects or detector calibration is small. The error on the overall detector energy scale is expected to be the dominant systematic error [14]. The large event rate in this experiment will allow us to measure Δm^2_{32} precisely in a short period of time; this measurement will be important to predict the shape of the appearance signal which we now discuss.

$\nu_\mu \rightarrow \nu_e$ Appearance

The importance of matter effects on long-baseline neutrino oscillation experiments has been recognized for many years [12, 22]. For our study, we have included the effect of matter with a full numerical calculation taking into account a realistic matter profile in the earth, following [23]. For our present discussion, it is useful to exhibit an approximate analytic formula for the oscillation of $\nu_\mu \rightarrow \nu_e$ for 3-generation mixing obtained with the simplifying assumption of constant matter density [24, 25]. Assuming a constant matter density, the oscillation of $\nu_\mu \rightarrow \nu_e$ in the Earth for 3-generation mixing is described approximately by Equation 1. In this equation $\alpha = \Delta m^2_{21}/\Delta m^2_{31}$, $\Delta = \Delta m^2_{31}L/4E$, $\hat{A} = 2VE/\Delta m^2_{31}$, $V = \sqrt{2}G_F n_e$. n_e is the density of electrons in the Earth. Recall that $\Delta m^2_{31} = \Delta m^2_{32} + \Delta m^2_{21}$. Also notice that $\hat{A}\Delta = LG_F n_e/\sqrt{2}$ is sensitive only to the sign of Δm^2_{31} .

$$\begin{aligned}
P(\nu_\mu \rightarrow \nu_e) \approx & \sin^2 \theta_{23} \frac{\sin^2 2\theta_{13}}{(\hat{A} - 1)^2} \sin^2((\hat{A} - 1)\Delta) \\
& + \alpha \frac{\sin \delta_{CP} \cos \theta_{13} \sin 2\theta_{12} \sin 2\theta_{13} \sin 2\theta_{23}}{\hat{A}(1 - \hat{A})} \sin(\Delta) \sin(\hat{A}\Delta) \sin((1 - \hat{A})\Delta) \\
& + \alpha \frac{\cos \delta_{CP} \cos \theta_{13} \sin 2\theta_{12} \sin 2\theta_{13} \sin 2\theta_{23}}{\hat{A}(1 - \hat{A})} \sin(\Delta) \cos(\hat{A}\Delta) \sin((1 - \hat{A})\Delta) \\
& + \alpha^2 \frac{\cos^2 \theta_{23} \sin^2 2\theta_{12}}{\hat{A}^2} \sin^2(\hat{A}\Delta)
\end{aligned} \tag{1}$$

For anti-neutrinos, the second term in Equation 1 has the opposite sign. It is proportional to the following CP violating quantity.

$$J_{CP} \equiv \sin \theta_{12} \sin \theta_{23} \sin \theta_{13} \cos \theta_{12} \cos \theta_{23} \cos^2 \theta_{13} \sin \delta_{CP} \tag{2}$$

Equation 1 is an expansion in powers of α . The approximation becomes inaccurate for $\Delta m_{32}^2 L/4E > \pi/2$ as well as $\alpha \sim 1$. For the actual results shown in Figure 2 we have used the exact numerical calculation, accurate to all orders. Nevertheless, the approximate formula is useful for understanding important features of the appearance probability: 1) the first 3 terms in the equation control the enhancement (for *NO*) or suppression (for *RO*) of the oscillation probability above 3 GeV; 2) the second and third terms control the sensitivity to CP in the intermediate 1 to 3 GeV range; and 3) the last term controls the sensitivity to Δm_{21}^2 at low energies.

While the ν_μ disappearance result will be affected mainly by systematic errors, the $\nu_\mu \rightarrow \nu_e$ appearance result will be affected by the backgrounds. The ν_e signal will consist of clean, single electron events (single showering rings in a water Cherenkov detector) that result mostly from the quasielastic reaction $\nu_e + n \rightarrow e^- + p$. The main backgrounds will be from the electron neutrino contamination in the beam and reactions that have a π^0 in the final state. The π^0 background will depend on how well the detector can distinguish events with single electron induced and two photon induced electromagnetic (e.m.) showers. Backgrounds due to $\nu_\mu \rightarrow \nu_\tau$ conversion, ν_τ charged current reactions in the detector, and subsequent $\tau^- \rightarrow e^- \bar{\nu}_e \nu_\tau$ decays are small because of the low energy of the beam and the consequent low cross section for τ production [14].

Because of the rapid fall in the BVLB neutrino spectrum beyond 4 GeV (Figure 3), the largest contribu-

tion to the π^0 background will come from neutral current events with a single π^0 in the final state. It is well known that resonant single pion production in neutrino reactions has a rapidly falling cross section as a function of momentum transfer, q^2 , [26] up to the kinematically allowed value. This characteristic alone suppresses this background by more than 2 orders of magnitude for π^0 (or shower) energies above 2 GeV [14]. Therefore a modest π^0 background suppression (by a factor of ~ 15 below 2 GeV and ~ 2 above 2 GeV) is sufficient to reduce the π^0 background to manageable level over the entire spectrum. The electron neutrino contamination in the beam from decays of muons and kaons, is well understood to be 0.7% of the muon neutrino flux [27], with a similar spectrum (Figure 3). The experimentally observed electron neutrino energy spectrum will therefore have three components: the rapidly falling shape of the π^0 background, the spectral shape of the ν_e beam contamination slightly modified by oscillation, and the oscillatory shape of the appearance signal. The shape of the appearance spectrum will be well known because of the precise knowledge of Δm_{32}^2 from the disappearance measurement as well as the improved knowledge of Δm_{21}^2 from KamLAND [5]. These distinguishing spectra will allow experimental detection of $\nu_\mu \rightarrow \nu_e$ with good confidence. Figure 6 shows a simulation of the expected spectrum of reconstructed electron neutrino energy after 5×10^7 sec of running. The parameters assumed are listed in the figure as well as the caption.

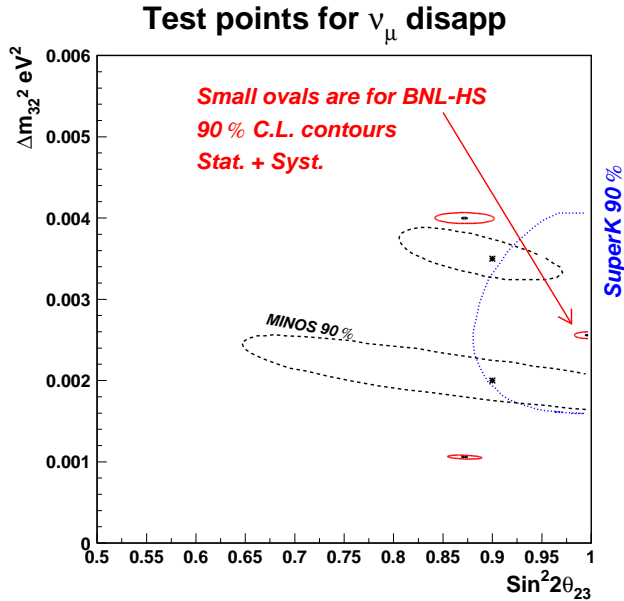


FIG. 5: (color) Resolution including statistical and systematic effects at 90% confidence level on Δm_{32}^2 and $\sin^2 2\theta_{23}$ for the 2540 baseline experiment; assuming 1 MW, 0.5 MT, and 5×10^7 sec of exposure. We have included a 5% bin-to-bin systematic uncertainty in the energy calibration as well as a 5% systematic uncertainty in the normalization. We have not included a systematic uncertainty on the global energy scale; this should be added in quadrature to the expected resolution on Δm_{32}^2 . The expected resolution from the MINOS experiment at Fermilab (dashed) and the allowed region from Super Kamiokande (dotted) is also indicated.

Figure 6 further illustrates the previously described three regions of the appearance spectrum: the high energy region (> 3 GeV) with a matter enhanced (for NO) appearance has the main contribution to the background from ν_e contamination in the beam; the intermediate region ($1 \rightarrow 3$ GeV) with high sensitivity to the CP phase, but little dependence on mass ordering, has approximately equal contribution from both background sources (ν_e and π^0); and the low energy region (< 1.5 GeV), where the effects of the CP phase and Δm_{21}^2 dominate, has the main background from the π^0 events. Matter enhancement of the oscillations has been postulated for a long time without experimental confirmation [12]. Detection of such an effect by observing a matter enhanced peak around 3 GeV will be important. However, in the case of RO mass ordering this enhanced peak will be missing, but the effect (depending on δ_{CP}) on the rest of the electron neutrino spectrum will be small.

The very long baseline combined with the low energy spectrum make it possible to observe $\nu_\mu \rightarrow \nu_e$ conversion even if $\sin^2 2\theta_{13} = 0$ because of the contribution from Δm_{21}^2 if the solar neutrino large mixing angle solution (LMA) holds. In Figure 7 we show the expected appearance spectrum for $\Delta m_{21}^2 = 7.3 \times 10^{-5} eV^2$ (LMA-I) with 90 excess events and $\Delta m_{21}^2 = 1.8 \times 10^{-4} eV^2$ (LMA-II) with 530 excess events above background. The LMA-I and LMA-II solutions with their respective confidence levels are discussed in [28]. This measurement will be sensitive to the magnitude and knowledge of the background because there will be no oscillating signature to distinguish the signal. We estimate that the statistical and systematic errors on this measurement will allow us to determine the combination $\Delta m_{21}^2 \times \sin 2\theta_{12}$ to a precision of about 10% at the LMA best fit point. This is competitive with the expected measurement from KamLAND. However, it will be done in the explicit ($\nu_\mu \rightarrow \nu_e$) appearance mode, which is qualitatively different from the measurements made so far in the SNO or the KamLAND experiments. Therefore, such a measurement will have important implications on the search for new physics such as sterile neutrinos.

In Figure 8 we show the 90 and 99.73% (3 sigma) C.L. sensitivity of the BVLB experiment in the variables $\sin^2 2\theta_{13}$ versus δ_{CP} . The actual limit obtained in the case of a lack of signal will depend on various ambiguities. Here we show the 99.73% C.L. lines for NO and RO , on the right hand of which the experiment will observe an electron appearance signal due to the presence of terms involving θ_{13} with greater than 3 sigma significance and thus determine the corresponding mass ordering. Currently from atmospheric data there is a sign uncertainty on $\theta_{23} = \pm\pi/4$; this introduces an additional ambiguity onto Figure 8 of $\delta_{CP} \rightarrow \delta_{CP} + \pi$. For this plot we have assumed that the other parameters are well known either through other experiment or by the disappearance measurement: $\Delta m_{21}^2 = 7.3 \times 10^{-5} eV^2$, $\Delta m_{32}^2 = 0.0025 eV^2$. The values of $\sin^2 2\theta_{12}$ and $\sin^2 2\theta_{23}$ are set to 0.86, 1.0, respectively. The sensitivity to $\sin^2 2\theta_{13}$ is approximately constant in the Δm_{32}^2 range allowed by Super Kamiokande [14]. The value of Δm_{21}^2 affects the modulation of the $\sin^2 2\theta_{13}$ sensitivity with respect to δ_{CP} . If there is no excess electron appearance signal, other than the expected signal due to Δm_{21}^2 alone, then it would indicate a switch to anti-neutrino running to determine if the RO hypothesis with parameters on the left hand side of the dashed line in Figure 8 applies [20].

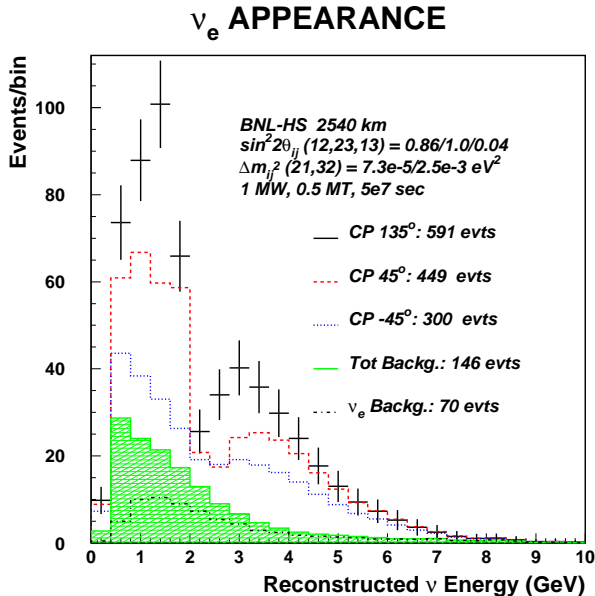


FIG. 6: (color) The expected electron neutrino spectrum for 3 values of the CP parameter δ_{CP} including background contamination. The points with error bars are for $\delta_{CP} = 135^\circ$; the error bars indicate the expected statistical error on each bin. The histogram directly below the error bars is for $\delta_{CP} = 45^\circ$ and the third histogram is for $\delta_{CP} = -45^\circ$. The hatched histogram shows the total background. The ν_e beam background is also shown. The plot is for $\Delta m_{32}^2 = 0.0025 \text{ eV}^2$. We have assumed $\sin^2 2\theta_{13} = 0.04$ and $\Delta m_{21}^2 = 7.3 \times 10^{-5} \text{ eV}^2$. The values of $\sin^2 2\theta_{12}$ and $\sin^2 2\theta_{23}$ are set to 0.86, 1.0, respectively. Running conditions as in Figure 4.

Sensitivity to the CP Violation Parameter

To get a qualitative understanding for the measurement of CP violating parameters we compare the size of terms involving δ_{CP} with the first term in Equation 1. This ratio is seen to be approximately proportional to $\alpha \sin \delta_{CP} (\Delta m_{21}^2 L / 4E_\nu)$. As shown in Figure 2, the fractional contribution from the CP violating terms increases for lower energies at a given distance. The energy dependence of the CP effect and the matter effect tend to be opposite and therefore can be distinguished from each other from the energy distribution using neutrino data alone. On the other hand, the statistics for a given size detector at a given energy are poorer by one over the square of the distance, but the term linear in $\sin \delta_{CP}$ grows linearly in distance [13]. The statistical sensitivity (approximately proportional to the square root of the event rate) to the effects of CP violation, therefore, is independent of distance because the loss of event rate

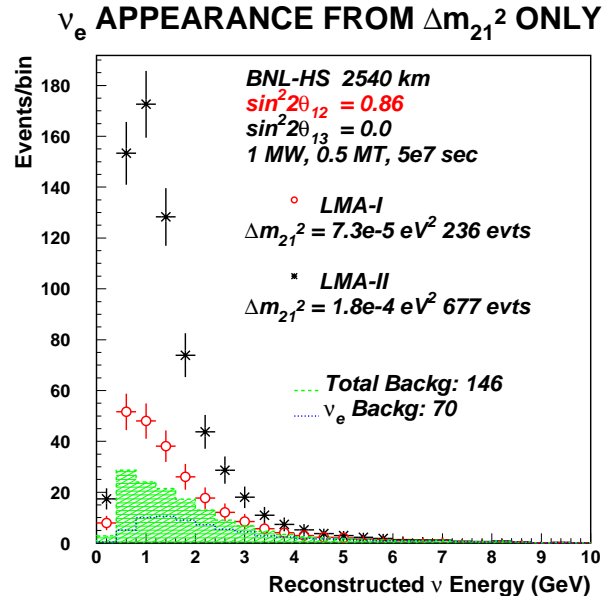


FIG. 7: (color) The expected spectrum of electron neutrino events for $\sin^2 2\theta_{13} = 0$. Important parameters in this figure are $\Delta m_{21}^2 = 7.3 \times 10^{-5} \text{ eV}^2$ (LMA-I) or $\Delta m_{21}^2 = 1.8 \times 10^{-4}$ (LMA-II) and $\sin^2 2\theta_{12} = 0.86$. All other parameters and the running condition as in Figure 4.

and the increase of the CP effect approximately cancel each other in the statistical merit if backgrounds remain the same. Therefore, the two important advantages of the BVLB approach are that the CP effect can be detected without running in the anti-neutrino mode and the sensitivity to systematic errors on the background and the normalization is considerably reduced because the fractional size of the CP effect is large. For example, in Figure 2, the CP effect at $\delta_{CP} = \pi/4$ in the first oscillation peak is $\sim 20\%$ while the effect in the second oscillation peak is more than 50%. Therefore, it is unnecessary to know the background and the normalization to better than 10% to obtain a significant measurement of δ_{CP} at the second oscillation maximum. There could be a contribution to the systematic error from the theoretical calculation of the probability shown in Figure 2. Because of the very long baseline, this probability depends on the Earth's density profile which is known to about 5%. Random density fluctuations on that order will lead to a relative systematic uncertainty in the ν_e appearance probability of about 1% [29], which is not significant for the BVLB method, but could be significant in the case of an experiment that performs the CP measurement at

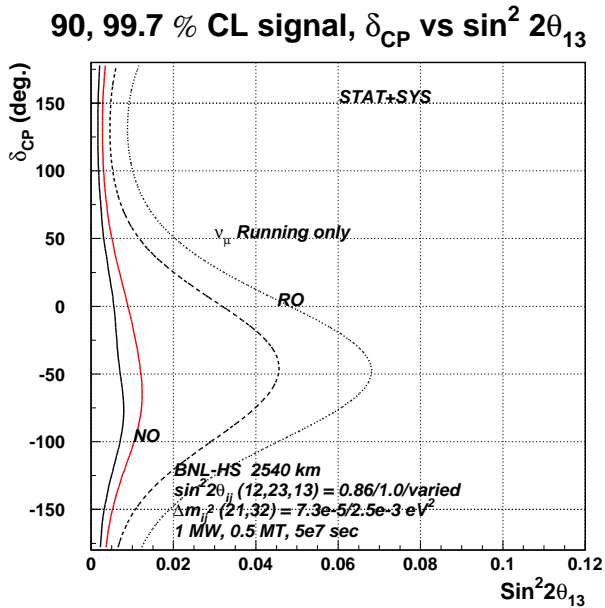


FIG. 8: (color) 90 and 99.73% C.L. contours of the BVLB experiment in the variables $\sin^2 2\theta_{13}$ versus δ_{CP} for the natural (*NO*) and reversed ordering of parameters (*RO*). The solid lines are for *NO*, the left line for 90% and right line for 99.73% C.L. The dashed and dotted lines are for 90 and 99.73% C.L. for *RO*. On the right hand side of the 99.73% C.L. lines the experiment will observe an electron appearance signal with greater than 3 sigma significance.

the first oscillation maximum with a shorter baseline.

An experiment with a wide band beam is needed to exploit the energy dependence of the CP effect to extract the value of δ_{CP} and $\sin^2 2\theta_{13}$ using only the neutrino data. The energy dependence also reduces the correlation between the two parameters. Figure 9 shows the expected resolution on $\sin^2 2\theta_{13}$ versus δ_{CP} at a particular case, $\sin^2 2\theta_{13} = 0.04$ and $\delta_{CP} = \pi/4$ with all other parameters fixed as indicated. The 1σ error on δ_{CP} from this measurement as a function of δ_{CP} is shown in Figure 10. It is clear that the precision of the measurement will be limited if $\sin^2 2\theta_{13} < 0.01$ because of the background. However, for larger values the resolution on δ_{CP} is approximately independent of $\sin^2 2\theta_{13}$. This result can be understood by examining Equation 1 in which the first term grows as $\sin^2 2\theta_{13}$ and the CP violating term grows as $\sin 2\theta_{13}$. Therefore the statistical sensitivity to the CP violating term, which is the ratio of the second term to the square-root of the first term, is independent of θ_{13} as long as the background does not dominate [13]. At $\delta_{CP} \approx 135^\circ$ the event rate reaches maximum and does

not change rapidly with respect to δ_{CP} , therefore the resolution on δ_{CP} becomes poor.

Because of the multiple node spectrum the appearance probability is sensitive to both the $\sin \delta_{CP}$ and $\cos \delta_{CP}$ terms in Equation 1. This eliminates the $\delta_{CP} \rightarrow (\pi - \delta_{CP})$ ambiguity normally present in a narrow band single node experiment [8]. The sign uncertainty $\theta_{23} = \pm\pi/4$ introduces a $\delta_{CP} \rightarrow (\delta_{CP} + \pi)$ ambiguity. If Δm_{21}^2 is known poorly, there will be a contribution to the δ_{CP} resolution due to the correlation between δ_{CP} and Δm_{21}^2 . We expect to know Δm_{21}^2 from KamLAND with precision of $< 10\%$ [5]; this does not introduce a dominant source of uncertainty on δ_{CP} in our experimental method. If a four parameter, Δm_{21}^2 , $\sin^2 2\theta_{12}$, $\sin^2 2\theta_{13}$, and δ_{CP} , fit to the data is performed, the correlations between the parameters dilute the sensitivity to each parameter. However, the ambiguities and correlations do not reduce the ability of the experiment to establish that 3-generation neutrino mixing contains a non-zero complex phase and hence a CP violating term. This is seen if we consider the resolution on the quantity $\Delta m_{21}^2 \times J_{CP}$ which is CP violating and by definition does not exhibit any of the above correlations. The measurement of this quantity will simply depend on the statistics in the low and medium energy components of the spectrum.

Comparison to Other Techniques

The alternatives to the BVLB plan fall into two categories: experiments with conventional horn focused beams over baselines of several hundred km and with beams based on neutrinos from muon decays in a high intensity muon storage ring. For a recent review of muon storage ring based neutrino factory physics as well as comparisons to conventional neutrinos beams see [30].

Recently, for the conventional beam an “off-axis” beam is preferred because the energy spectrum is narrower and can be tuned, within a limited range from 1 to 2 GeV by choosing the off-axis angle [6]. A narrow energy spectrum could be better suited for identifying $\nu_\mu \rightarrow \nu_e$ conversion because the neutral current backgrounds from interactions of high energy neutrinos are lowered. The JPARC to Super Kamiokande project (baseline of 295 km) has adapted this strategy and a new initiative at Fermilab based on the NuMI beamline (baseline of 732 km) is also considering it [7]. Both of these projects focus on the observation of a non-zero value for θ_{13} . Since it is not pos-

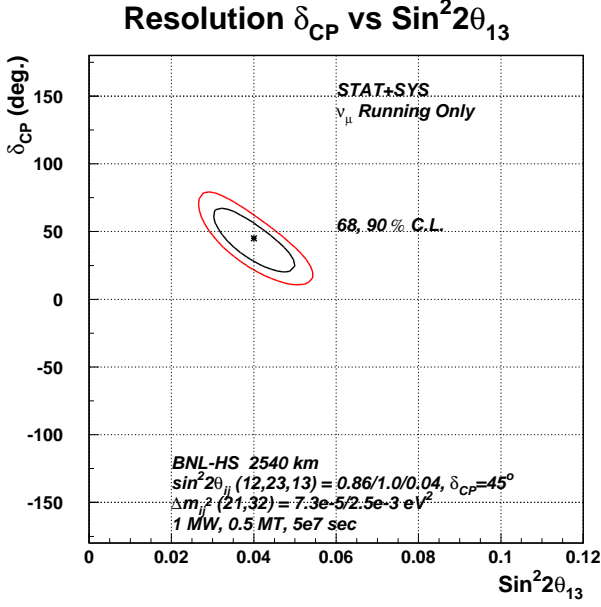


FIG. 9: (color) 68% and 90% confidence level error contours in $\sin^2 2\theta_{13}$ versus δ_{CP} for statistical and systematic errors. The test point used here is $\sin^2 2\theta_{13} = 0.04$ and $\delta_{CP} = 45^\circ$. $\Delta m_{32}^2 = 0.0025 \text{ eV}^2$, and $\Delta m_{21}^2 = 7.3 \times 10^{-5} \text{ eV}^2$. The values of $\sin^2 2\theta_{12}$ and $\sin^2 2\theta_{23}$ are set to 0.86, 1.0, respectively.

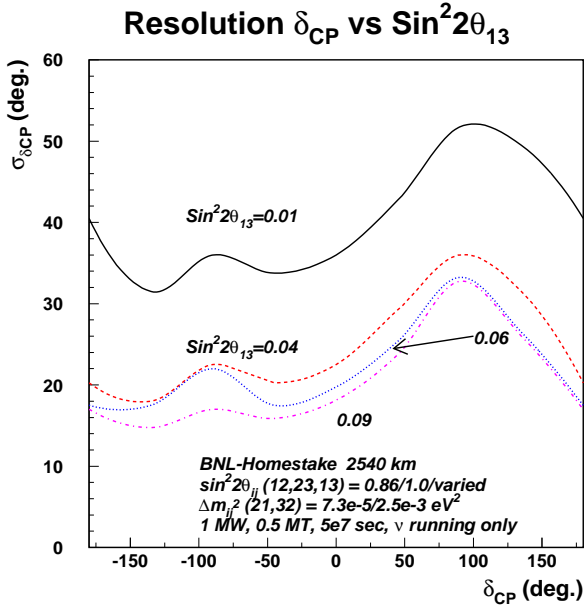


FIG. 10: (color) 1 sigma error on δ_{CP} in degrees for several values of $\sin^2 2\theta_{13}$. All other parameters are held fixed assuming they will be known before this measurement.

sible to eliminate the $\sim 0.5\%$ ν_e contamination in a conventional ν_μ beam (even if it is “off-axis”) the sensitivity of all projects based on a conventional beam, including the BVLB plan, is limited to $\sin^2 2\theta_{13} \sim 0.005$ (ignoring the effect of δ_{CP}). Sensitivity below this value is background limited and requires very good understanding of the systematic errors associated with the purity of the beam. The BVLB plan does, however, extend this sensitivity to values of Δm^2 down to 0.001 eV^2 . The “off-axis” projects must be upgraded to several Megawatts of beam power and detectors of several hundred kT (the second phase of the JPARC project calls for 4 MW beam and a 1 megaton detector) to perform the CP measurement. The narrow band nature of the beam requires running in the anti-neutrino mode to observe CP violation. The BVLB plan uses a wide band beam over a much longer distance to achieve the same sensitivity to $\sin^2 2\theta_{13}$ over a wider range of Δm_{32}^2 . It also has the ability to see a multiple node structure in both the disappearance and appearance channel; thus making the observation of $\nu_\mu \rightarrow \nu_e$ experimentally more robust against unanticipated backgrounds. In addition, the unique aspect of the wide band beam over the very long baseline is the ability to measure δ_{CP} with few ambiguities using neutrino data alone.

The muon storage ring based “neutrino factory” solves the background problem faced with conventional beams. A $\bar{\nu}_\mu$ and a ν_e is produced in each μ^+ decay. An appearance search looks for the conversion of ν_e into ν_μ by looking for events with negatively charged μ^- particles in the presence of $\bar{\nu}_\mu$ charged current events with positively charged μ^+ particles in the final state. Such a physics signature should potentially have very low background. Therefore, a neutrino factory based $\nu_e \rightarrow \nu_\mu$ search is estimated to be sensitive to $\sin^2 2\theta_{13}$ perhaps as small as $10^{-4} - 10^{-5}$. Such a facility is very well tuned for measurement of $\sin^2 2\theta_{13}$. Nevertheless, because of the relatively narrow energy spectrum and higher energy of the neutrino factory, it lacks the ability to observe multiple nodes in the observed spectrum. For the neutrino factory the effects of CP violation are observed by comparing $\bar{\nu}_e \rightarrow \bar{\nu}_\mu$ and $\nu_e \rightarrow \nu_\mu$ in two different runs of μ^- and μ^+ decays in the presence of very large matter effects. The narrow spectrum also limits the ability of the neutrino factory to resolve the ambiguities in the δ_{CP} determination regardless of the value of $\sin^2 2\theta_{13}$. This has been extensively discussed in the literature [8, 25] and one of the proposed solutions is to construct several detectors with different baselines to uniquely deter-

mine δ_{CP} versus $\sin^2 2\theta_{13}$. Although the neutrino factory can extend the reach for $\sin^2 2\theta_{13}$ to very small values because the backgrounds to the appearance search are small, the resolution on δ_{CP} – disregarding the ambiguities inherent in the neutrino factory approach – is comparable to the BVLB resolution. We therefore conclude, that if $\sin^2 2\theta_{13} \geq 0.01$ the BVLB experiment is either equal to or exceeds the physics reach for neutrino mixing parameters of the neutrino factory.

Other suggestions in the literature include ν_e or $\bar{\nu}_e$ beams from either decays of radioactive nuclei accelerated to high energies (beta-beam) [31] or $\bar{\nu}_e$'s from nuclear power generation reactors such as the beam used for KamLAND [5]. Both of these concepts aim to create very pure, but low energy beams. For CP sensitivity both ν_e and $\bar{\nu}_e$ must be produced in separate runs in the beta-beam concept. The low background should enable the beta-beam concept to have good sensitivity to θ_{13} , if sufficient flux can be obtained. The reactor beams are below ν_μ charged current reaction threshold and therefore must rely on disappearance to search for a non-zero value of θ_{13} . A disappearance based search for θ_{13} will most likely be limited by systematic errors. Further comments on these techniques must await more detailed studies.

Conclusions

We have simulated and analyzed a feasible, very long baseline neutrino oscillation experiment consisting of a low energy, wide band neutrino beam produced by 1 MW of 28 GeV protons incident on a carbon target with magnetic horn focusing of pions and kaons, and a 500 kT detector at a distance of > 2500 km from the neutrino source. The BVLB neutrino beam with a total intensity of about $4.7 \times 10^{-5} \nu/m^2/POT$ at a distance of 1 km from the target could be provided by an upgrade to the BNL-AGS [17].

The single BVLB experiment could produce measurements of all parameters in the neutrino mixing matrix through observation of the disappearance channel, $\nu_\mu \rightarrow \nu_\mu$ and the appearance channel, $\nu_\mu \rightarrow \nu_e$. The experiment is also sensitive to the mass ordering of neutrinos using the observation of the matter effect in the appearance channel through the currently unknown parameter $\sin^2 2\theta_{13}$. Nevertheless, the experiment is intended primarily to measure the strength of CP invariance violation in the neutrino sector and will provide a

measurement of the CP phase, δ_{CP} or alternatively the CP violating quantity, J_{CP} , if the one currently unknown neutrino oscillation mixing parameter $\sin^2 2\theta_{13} \geq 0.01$, a value about 15 times lower than the present experimental upper limit. We point out that for a given resolution on δ_{CP} the number of neutrino events needed which determines the detector size and beam intensity, is approximately independent of the baseline as well as the value of $\sin^2 2\theta_{13}$ as long as the electron signal is not background dominated. Therefore, the concept of very long baseline (≥ 2000 km) is attractive because it provides access to much richer physics phenomena as well as reduces the need to understand systematic errors on the flux normalization and background determination. A shorter baseline (< 1500 km) will obviously limit the reach of the experiment for $\Delta m_{21}^2 \times \sin 2\theta_{12}$ in the appearance mode as well as reduce the resolution on the CP parameter. On the other hand, a much longer baseline (> 4000 km) will result in a matter effect that is large enough to dominate the spectrum and make the extraction of the CP effect more difficult. The larger distance will also make it necessary to make the neutrino beam directed at a higher angle into the Earth, a technical challenge that may not be necessary given the current values of neutrino parameters. Lastly, we have also shown that most of this rich physics program including the search for CP effects can be carried out by neutrino running alone. Once CP effects are established with neutrino data, anti-neutrino data could be obtained for more precision on the parameters or search for new physics. The shape of the disappearance signal over multiple oscillations from neutrino running alone (as well as in combination with anti-neutrino running) can be used to constrain effects of new physics from: sterile neutrino mixing, extra dimensions, exotic interactions with matter, etc.

It has not escaped our notice that the large detector size (≥ 500 kT), mandated by the above described neutrino program, naturally lends itself to the important physics of proton decay, supernova detection, etc. Although some experimental requirements such as shielding from cosmic rays, detector shape, or photo-sensor coverage, may differ, it is clear that they can be resolved so that this large detector can also be employed to address these frontier physics issues.

I. ACKNOWLEDGEMENTS

We thank all contributors to the BNL neutrino working group, as well as the BNL-AGS technical staff and engineers whom we consulted during this work. We especially thank Thomas Roser, Nick Tsoupas, Alessandro Rug-

giero, Deepak Raparia, Nick Simos, and Hans Ludewig for their contribution to the accelerator and beam design. We also thank Thomas Kirk who encouraged us throughout this work. This work was supported by DOE grant DE-AC02-98CH10886 and NSF grant PHY02-18438.

-
- [1] PDG, Phys. Rev. **D66**, 010001 (2002), p. 281.
- [2] Y. Fukuda et al., Phys. Rev. Lett. **81**, 1562 (1998); S. Fukuda et al., Phys. Rev. Lett. **86** 5656, 2001; E.W. Beier, Phys. Lett. **B283**, 446 (1992); T. Kajita and Y. Totsuka, Rev. Mod. Phys. **73**, 85 (2001).
- [3] Q. R. Ahmad et al., Phys. Rev. Lett. **87** 071301 (2001). S. Fukuda et al., Phys. Rev. Lett., **86** 5651 (2001).
- [4] S. H. Ahn et al., Phys. Lett. **B 511** 178 (2001).
- [5] K. Eguchi, *et. al*, Phys. Ref. Lett. **90**, 021802 (2003). hep-ex/0212021.
- [6] The “off-axis” neutrino beam was first proposed by the E889 Collaboration, Physics Design Report, BNL No. 52459, April, 1995. <http://minos.phy.bnl.gov/nwg/papers/E889>.
- [7] The JHF-Kamioka neutrino project, Y. Itow et al., arXiv:hep-ex/0106019, June 2001. Letter of Intent to build an Off-axis Detector to study numu to nue oscillations with the NuMI Neutrino Beam, D. Ayres *et al.*, hep-ex/0210005.
- [8] V.D. Barger, S. Geer, R. Raja, K. Whisnant, Phys. Rev. D63: 113011 (2001); V. Barger et al., hep-ph/0103052; P. Huber, M. Lindner, W. Winter, Nucl. Phys. B645, 3 (2002); V. Barger, D. Marfatia, K. Whisnant, Phys. Rev. D65: 073023 (2002).
- [9] C. Albright et al., Physics at a Neutrino Factory; hep-ex/0008064; N. Holtkamp et al., Feasibility Study of a Neutrino Source Based on a Muon Storage Ring, FERMILAB-PUB-00-108-E *June 2000); S. Ozaki, R. Palmer, M. Zisman, and J. Gallardo, eds. Feability Study II of a Muon-Based Neutrino Source, BNL-52623 (2001) and references therein to other neutrino factory studies.
- [10] V.D. Barger, J.G. Learned, S. Pakvasa, T.J. Weiler, Phys.Rev.Lett.82:2640,(1999).
- [11] R. Barbieri, P. Creminelli, A. Strumia, Nucl.Phys.B585:28 (2000).
- [12] L. Wolfenstein in Proc. Neutrinos '78, Long-Distance Neutrino Detection (1978), p.108-112.
- [13] W. Marciano, hep-ph/0108181, 22 Aug. 2001.
- [14] D. Beavis *et al.*, Report of the BNL neutrino working group, BNL-69395, hep-ex/0211001.
- [15] Megaton Modular Multi-Purpose Neutrino detector, 3M collaboration, <http://www.hep.upenn.edu/Homestake>
- [16] Physics Potential and Feasibility of UNO, UNO collaboration, June 2001, Stony Brook University, SBHEP01-03.
- [17] J. Alessi *et al.*, AGS Super Neutrino Beam Facility, Accelerator and Target system Design, BNL-71228-2003-IR. April 15, 2003. <http://nwg.phy.bnl.gov/>
- [18] Accelerator Technical Design Report for High-Intensity Proton Accelerator Facility Project, Japan Atomic Energy Research Institute and High Energy Accelerator Research Organization, 2002. <http://j-parc.jp/>
- [19] The Proton Driver Design Study, Edited by W. Chou, C. Ankenbrandt and E. Malamud, FERMILAB-TM-2136, Dec. 2000.
- [20] If the value of $\sin^2 2\theta_{13}$ turns out to be too small or the true mass ordering is RO , then a switch to antineutrino data-taking would be indicated. Should a moderate amount of antineutrino data show a peak in the positron spectrum, then we can conclude that the RO hierarchy ($m_2 > m_1 > m_3$) holds true. If the neutrino data shows that the NO hierarchy is correct and that the CP parameter is non-zero, then we could switch to antineutrino data to explicitly show CP non-conservation and measure the parameters more precisely. The event rate for an anti-neutrino beam running for the same running time of 5×10^7 sec is about 19,000 charged current and 6000 neutral current events.
- [21] Numi MINOS project at Fermi National Accelerator Laboratory, <http://www.numi.fnal.gov/>
- [22] J. Arafune, M. Koike, and J. Sato, Phys. Rev. D56, 3093 (1997); erratum, *ibid*, D60, 119905 (1999).
- [23] I. Mocioiu and R. Shrock, Phys. Rev. **D62**, 053017 (2000); Snowmass e-Conf C 0106063 (June 2001), JHEP 0111, 050 (2001).
- [24] M. Freund, Phys.Rev. D64 (2001) 053003; M. Freund, P. Huber, M. Lindner, Nucl.Phys. B615 (2001) 331-357;
- [25] A. Cervera, *et al.*, Nucl. Phys. B579(2000) 17.
- [26] S.L. Adler, Annals of Physics 50 (1968) 189; D. Rein, L.M. Sehgal, Annals of Physics 133 (1981) 79.
- [27] L.A. Ahrens et al., Phys.Rev.D34:75, (1986). L.A. Ahrens *et al.*, Phys. Rev. **D41**, 3297 (1990)
- [28] G.L. Fogli, E. Lisi, A. Marrone, D. Montanino, A. Palazzo, A.M. Rotunno, hep-ph/0212127, Feb 5, 2003.
- [29] B. Jacobsson, T. Ohlsson, H. Snellman and W. Winter, Phys. Lett. B **532**, 259 (2002). hep-ph/0112138.
- [30] Oscillation Physics With a Neutrino Factory, M. Apolloio et al., CERN-TH/2002-208, hep-ph/0210192.
- [31] P. Zucchelli, Phys.Lett.B532:166-172,2002